Acta Neuropathol (2000) 100:205–212

REGULAR PAPER

J. Marksteiner · T. Lechner · W. A. Kaufmann
P. Gurka · C. Humpel · C. Nowakowski · H. Maier
K. A. Jellinger

Distribution of chromogranin B-like immunoreactivity in the human hippocampus and its changes in Alzheimer's disease

Received: 14 February 2000 / Accepted: 6 March 2000

Abstract Synapse loss is crucially involved in cognitive decline in Alzheimer's disease (AD). This study was performed to investigate the distribution and density of chromogranin B-like immunoreactivity in the hippocampus of control compared to AD brain. Chromogranin B is a large precursor molecule found in large dense-core vesicles. For immunocytochemistry we used an antiserum raised against a synthetic peptide (PE-11) present in the chromogranin B molecule. Chromogranin B-like immunoreactivity was concentrated in the terminal field of mossy fibers, the inner molecular layer of the dentate gyrus and in layer II of the entorhinal cortex. In AD, chromogranin B was detected in neuritic plaques. The density of chromogranin B-like immunoreactivity was significantly reduced in the inner molecular layer of the dentate gyrus and in layers II, III and V of the entorhinal cortex in AD brains. The present study demonstrates that chromogranin B is a marker for human hippocampal pathways. It is particularly suitable for studying nerve fibers terminating at the inner molecular layer of the dentate gyrus. It is present in neuritic plaques, and its density is reduced in a layer-specific manner.

Key words Human brain · Hippocampus · Alzheimer's disease · Chromogranin B · Synapse loss

J. Marksteiner (✉) · T. Lechner · W. A. Kaufmann · P. Gurka
C. Humpel · C. Nowakowski
Department of Psychiatry, University of Innsbruck,
Anichstrasse 35, 6020 Innsbruck, Austria
e-mail: j.marksteiner@uibk.ac.at,
Tel.: +43-512-5043712, Fax: +43-512-5043713

H. Maier
Department of Pathology, University of Innsbruck, Austria

K. A. Jellinger
Ludwig-Boltzmann-Institute of Clinical Neurobiology,
Vienna, Austria

Introduction

Progressive impairment in memory and cognition is a clinical key feature of Alzheimer's disease (AD), but the pathogenesis of the lesions leading to cognitive decline is not well understood. AD is morphologically characterized by the presence of neurofibrillary tangles and senile plaques. Loss of neurons and loss of synapses are of principal importance in intercellular communication in neural circuits in AD [26]. Correlation of synaptic and pathological markers with cognition of the elderly suggests that cytoskeletal alterations are important in AD [7].

Chromogranin B belongs to the chromogranins which include chromogranin A, chromogranin B [15], secretogranin II, and 7B2 [24]. Chromogranins are found in large dense-core vesicles throughout the endocrine and nervous tissue [9]. They are stored together with different peptide hormones and neuropeptides. Neuropeptides are soluble constituents of large dense-core vesicles. They are differentially affected in AD [6, 14]. For example, the concentration of somatostatin is reduced both in the brain tissue and cerebrospinal fluid [34]. In AD there are dramatic reductions in human corticotropin-releasing factor concentration and reciprocal increases in CRF receptor density in the cortex [1]. Other neuropeptides, such as vasoactive intestinal polypeptide, are not changed [12, 37].

The molecular properties and the distribution of secretogranin II and chromogranin A are better characterized than those of chromogranin B. Chromogranin A and B mRNA have been detected in pyramidal neurons of human cerebral cortex by in situ hybridization histochemistry [8]. Several peptides derived from chromogranin B have been demonstrated in various tissues [2]. Recently, we performed a detailed immunohistochemical mapping for chromogranin B in rat brain, and investigated the degree of proteolytic processing [22] using an antibody generated against a synthetic peptide (PE-11) derived from the chromogranin B sequence. Our results demonstrated a significant processing of chromogranin B as well as its widespread and distinct distribution [22]. In human brain,

PE-11-like immunoreactivity (PE-11-LI) is strongly concentrated in several areas including the bed nucleus of the stria terminalis, hippocampus, hypothalamus, and different brain stem nuclei [25].

There were several objectives for the present study. Firstly, we intended to investigate whether chromogranin B-LI is present in the human hippocampal formation, the subiculum and the entorhinal cortex. A detailed immunocytochemical study may reveal which hippocampal pathways contain this peptide. We were particularly interested in whether chromogranin B-LI is found, as in the rat, in a high concentration in the inner molecular layer of the dentate gyrus. In the second part of the present study, the staining pattern of chromogranin B-LI was investigated in AD. A main objective was to determine whether chromogranin B is present in neuritic plaques and if so, how the distribution of chromogranin B-containing plaques correlates with that of chromogranin B-LI. In addition, we studied the density of chromogranin B-LI in the different parts of the hippocampus and entorhinal cortex in AD compared to age-matched controls.

The main goal of the present study was to establish a further neuronal marker for the hippocampal pathways in man, and to provide a neuroanatomical baseline for changes in AD.

Methods and materials

Control subjects

The brains of seven adult humans (three males and four females; average age 76.5 ± 8.4 years), with no known neurological or psychiatric disease, were obtained at routine autopsy at a postmortem interval of 17 ± 3.5 h. Hospital and other medical records confirmed that these subjects had normal intellectual function until the time of their deaths (Table 1). Histologically three brains displayed very rare neocortical plaques, but no neocortical tangles. In four control cases a small number of plaques was detected in the subiculum.

Alzheimer's disease

Five patients fitting the NINCDS-ADRDA clinical criteria of AD were included [27]. Average age was 79.4 ± 6.5 years. The postmortem interval was 19.5 ± 4.2 h. Neuropathological examination used standardized protocols [17, 18] and included the following criteria: NIA [20, 36]; CERAD [28]; staging of neuritic plaques [3] and the recent NIA-RI classification [16]. Diffuse Lewy body disease, Pick disease, multi-infarct dementia, and other causes of dementia were excluded.

Antiserum

The generation of the PE-11 antiserum was described previously [22]. Briefly, it was generated against a synthetic peptide (PE-11) corresponding to rat chromogranin B 552–562 [11] which is identical with the human sequence. The antiserum only reacts with the free C-terminal part of PE-11 since an elongated peptide (chromogranin B 552–574) only reacts in the radioimmunoassay (RIA) when it is first subjected to trypsin digestion [22]. No cross-reactivity was found with peptides derived from chromogranin A and secretogranin II or with the following neuropeptides: galanin, substance P, neuropeptide Y, neurotensin and calcitonin gene-related peptide.

Tissue preparation for histological analysis

Tissue blocks containing the caudal amygdala, the entire hippocampus and entorhinal cortex were dissected. They were cut into coronal slices, about 1 cm thick, and immediately fixed by immersion in cold 4% paraformaldehyde in sodium phosphate buffer (PBS), pH 7.2, for 1 week. One block was dehydrated in graded ethanols, embedded in paraffin and cut serially in 3-µm-thin coronal sections. The remaining slices were rinsed in PBS for 1 day, and were sequentially transferred to 5%, 15% and 20% sucrose in PBS for 1 day each. These slices were frozen in isopentane (–45 °C) for 3 min and stored at –70 °C. Free-floating sections were prepared using a freezing microtome.

Chromatographic analysis of chromogranin B-LI at different postmortem intervals

Samples (~ 150 mg each) of the hippocampus were dissected from brains 4, 8, 16, 24, 32, and 48 h after death. Two cases per time point were used. Samples were immediately frozen in isopentane (–50 °C) and stored until use at –70 °C in a biofreeze. Chromatographic analysis was performed as previously described [26]. Gel filtration fractions were further analyzed by reverse-phase high-pressure liquid chromatography. Fractions were collected and subjected to RIA [26].

Table 1 Information about the patients from whom brains were obtained. GDS stage [30]: *1* no cognitive decline, *6* severe cognitive decline, *7* very severe cognitive decline; MME as defined in [10] (*GDS* Global Deterioration Scale, *MME* Mini Mental State Examination)

Sex	Age (years)	GDS	MME	Braak	Cause of death	Brain weight (g)
M	71	1	28	–	Myocardial infarction	1,250
M	71	1	27	–	Aspiration pneumonia	1,310
F	87	1	27	–	Liver cancer	1,274
F	70	1	28	–	Traffic accident	1,220
M	87	1	27	–	Pulmonary embolism	1,280
F	68	1	27	–	Myocardial infarction	1,300
M	82	1	29	–	Pulmonary embolism	1,290
Braak V–VI						
F	85	7	12	VI	Myocardial infarction	1,260
F	75	7	7	V	Pneumonia	1,040
M	72	6	13	VI	Rupture of aorta	1,120
M	87	7	8	V	Pneumonia	1,040
F	76	7	4	VI	Liver cancer	850

Immunocytochemistry for chromogranin B-LI

Every tenth section (coronal and sagittal; 40 μm) was stained for PE-11. Adjacent sections were stained with a monoclonal mouse antibody to human β-amyloid (anti-β/A4; 6F/3D; Dako, Glostrup, Denmark; dilution 1:80). Free-floating sections were processed according to the avidin-biotin-peroxidase complex (ABC) method as previously described in detail [26]. Briefly, free-floating sections were rinsed several times in 50 mM TRIS-HCl-buffered saline (TBS) containing 0.4% Triton X-100 (TBS-T), pH 7.2, for 3 h. Endogenous peroxidase activity was blocked with 0.9% H_2O_2 and 20% methanol in TBS for 30 min, and sections were rinsed in TBS-T again (three times 10 min each). After incubation with 10% normal goat serum (Bender, Vienna, Austria) in TBS-T to block nonspecific binding sites, sections were incubated with primary antiserum (anti-PE-11: 1:3,000) in TBS-T for 38 h at 4 °C. After rinsing in TBS-T (three times 10 min each), sections were processed with biotinylated secondary antibodies (biotinylated goat anti-rabbit IgG; 1:200 in TBS-T; Vector, Burlingame, USA) and rinsed in TBS-T again (three times 10 min each). Afterwards, sections were processed with ABC solution (1:200 in TBS-T; Vector) for 90 min each at room temperature and rinsed in TBS (four times 10 min each). The sections were reacted with 0.05% 3,3′-diaminobenzidine (Sigma, Munich, Germany) and 0.003% H_2O_2 in TBS for 6–7 min, rinsed in TBS several times, mounted on chromalaun-gelatine-coated glass slides, air dried and covered with entellan. Bovine serum albumin was added to all antibody dilutions (1%) and the ABC (0.1%). Controls without primary antiserum and antisera preadsorbed with the synthetic secretoneurin peptide (10 μM, 24 h, 4 °C) were included in each experiment.

All sections were examined with light microscope (Axiophot, Zeiss, Austria). Photomicrographs were taken with the same microscopical equipment.

Immunocytochemistry with paraffin-embedded sections

Briefly, sections were rehydrated in a series of ethanols, and were incubated with an antibody against chromogranin B (1:600) in TBS pH 7.2 for 48 h at 4 °C. After rinsing in TBS, sections were processed with biotinylated secondary antibodies (biotinylated goat anti-rabbit IgG; 1:75 in TBS-T; Vector) and rinsed in TBS again (three times 10 min each). Afterwards, sections were processed with ABC (1:75 in TBS; Vector) for 90 min each at room temperature and rinsed in TBS (four times 10 min each). The sections were reacted with 0.05% 3,3′-diaminobenzidine (Sigma). The reaction was terminated by washing the sections in TBS. They were then dehydrated, cleared in xylene and coverslipped.

Quantitative and statistical analysis

The density of chromogranin B immunostaining was assessed in the inner and outer molecular layer of the dentate gyrus, granule cell layer, hilus, CA3, CA1 subregions of the Ammon's horn, and various layers of the entorhinal cortex in both controls and AD brains. An image-pro analysis system (Media Cybernetics, Silver Spring, USA) linked to an Olympus light microscope via a CCD video camera was used to determine the density of immunostaining; 8-bit gray scale images of immunostained sections were taken at ×200. Intensity values of transmitted light representing the maximal optical density (OD-max) and minimal optical density (OD-min) were calibrated to the image before measuring the density of immunostaining: OD-min = 0.004 (white) and OD-max = 2.406 (black).

The density of chromogranin B-LI was determined in respective layers on ten consecutive sections per case. A mean optical

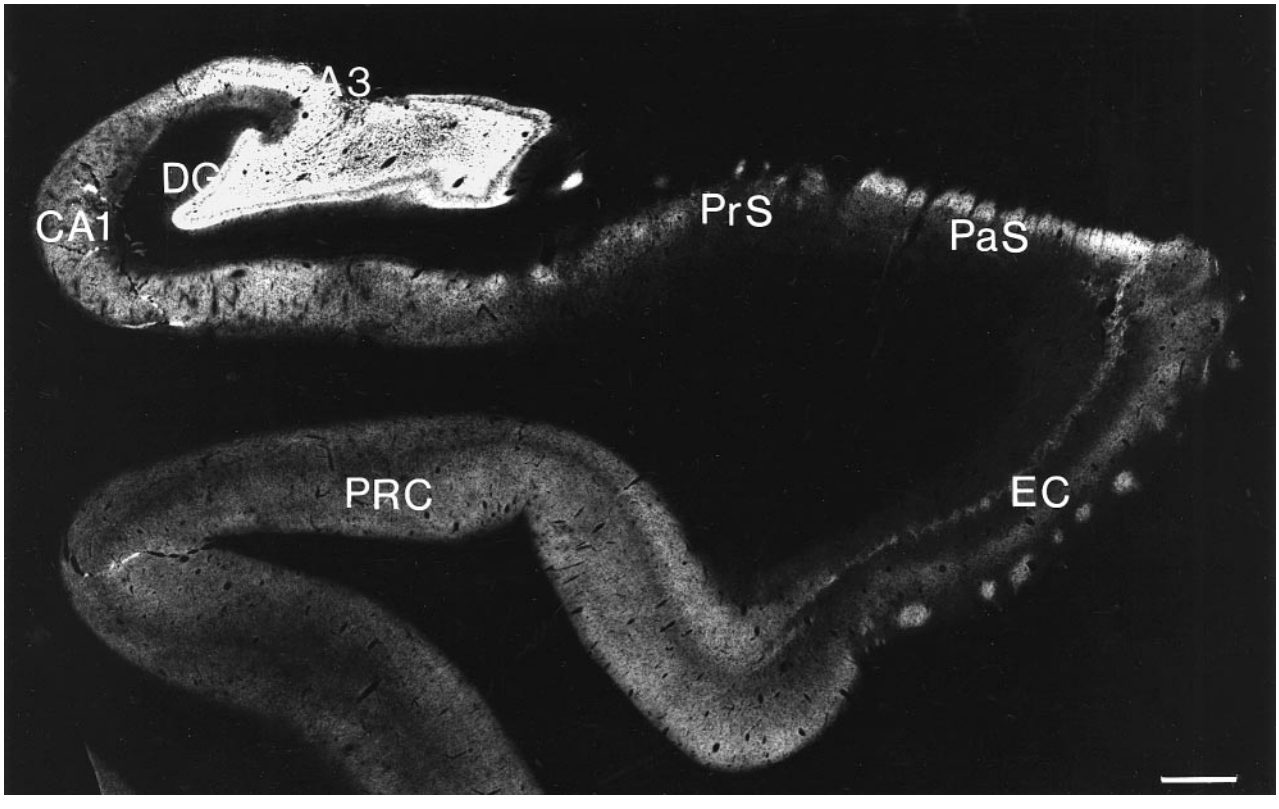

Fig. 1 Chromogranin B-LI is shown in a representative, coronal section of the human hippocampal formation and parahippocampal gyrus. The picture was obtained using an immunostained section as a negative in a photographic enlarger, thus immunoreactive structures appear white. A high density of chromogranin B-LI is observed in the dentate gyrus (*DG*), CA3, the pre (*PrS*) and parasubiculum (*PaS*) and the entorhinal cortex (*EC*) (*chromogranin B-LI* chromogranin B-like immunoreactivity, *PRC* perirhinal cortex). *Bar* 1.5 mm

density (gray level) was then calculated for each layer from all sections of each case.

Statistical analysis was performed by means of the Statistica v4.0 program (Statsoft, Inc.). Statistical comparison between patients with AD and controls was done using the Mann-Whitney U-test.

Results

Distribution of chromogranin B-LI in controls

Chromatographic analysis of different postmortem intervals (4, 8, 16, 24, 32, 48 h) revealed no change in the chromatographic profile up to 48 h (data not shown) (longer intervals were not investigated), indicating a high stability of the PE-11 peptide under postmortem conditions.

The highest density of chromogranin B-LI was found in the terminal field of mossy fibers, in the inner molecular layer of the dentate gyrus and in the entorhinal cortex (Fig. 1).

The hippocampus displayed a high density of chromogranin B-LI in the hilus and stratum lucidum of the CA3 area due to the very intense staining of mossy fibers (Fig. 2 A). Immunopositive cells were observed in the granule cell layer (Fig. 3 C) that was transversed by immunoreactive fibers. A few perikarya were present in the hilus. The inner molecular layer of the dentate gyrus was intensely immunopositive throughout the hippocampal formation. Chromogranin B-LI appeared as varicose fibers and as differently sized varicosities (Fig. 3 C). The outer molecular layer displayed a clearly lower density of immunoreactivity than the inner molecular layer (Fig. 3 C).

In general, neurons of the principal cell layer of CA3, CA2 and CA1 were chromogranin B immunopositive. They were often surrounded by chromogranin B-immunoreactive varicosities. In CA3, the stratum lucidum was covered by the intensely stained mossy fibers, which increased in intensity at the border with the CA2 sector (Fig. 2 A). In CA1, scattered chromogranin B-immunopositive neurons were present. In the stratum radiatum, chromogranin B-immunoreactive fibers were oriented perpendicularly to the CA1 principal cell layer.

The subiculum contained chromogranin B-LI cells and varicose fibers. In the presubiculum and parasubiculum, a high density of chromogranin B was found consisting of varicose fibers and terminals (Fig. 1).

The entorhinal cortex displayed a very high density of chromogranin B-LI (Fig. 1). Immunoreactivity was particularly strong in layer II, layer III and layer V (Fig. 3 A). Chromogranin B-LI mainly consisted of differently sized varicosities in layer II and in layer III. In layer V varicose fibers predominated.

Chromogranin B-LI in AD

The overall staining pattern of chromogranin B was characterized (i) by the appearance of chromogranin B-containing plaques (Fig. 2 B), and (ii) by a decrease in density of chromogranin B-LI (Figs. 2–5). The highest numbers of chromogranin B-immunopositive plaques were detected in the entorhinal cortex followed in decreasing order by subiculum (Fig. 4 A), the CA1 and CA2 sector, and the molecular layer of the dentate gyrus. Neuritic plaques containing dystrophic chromogranin B-immunopositive elements predominated (Fig. 4 B). In general, about 15–

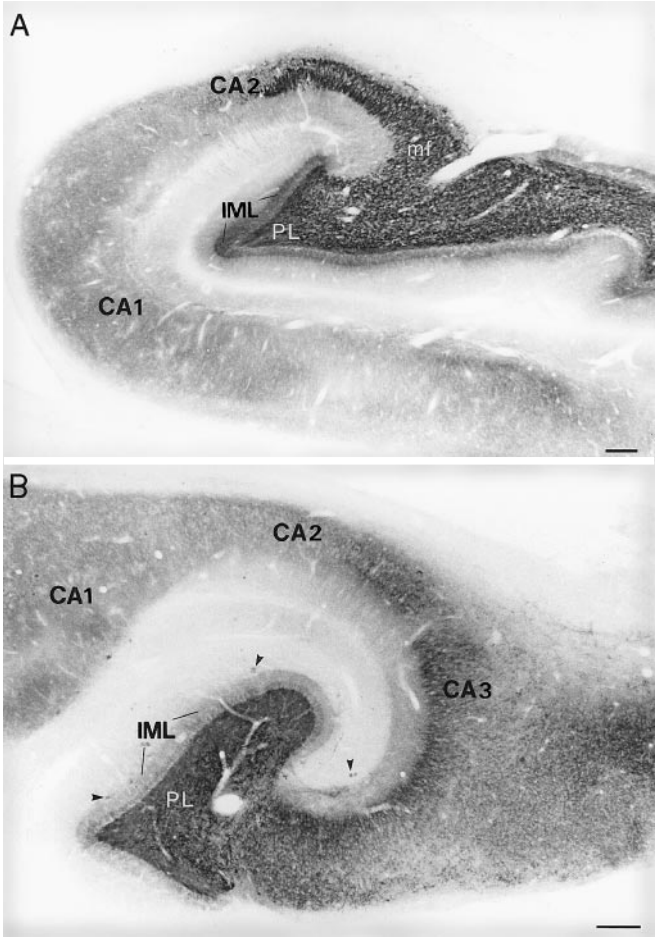

Fig. 2 In the hippocampal formation chromogranin B-LI is shown in coronal sections of controls (**A**) and in sagittal sections of AD (**B**). A high density of chromogranin B-LI is found in the terminal field of mossy fibers (*mf*), CA2 and CA1 area. Chromogranin B-LI is significantly reduced in inner molecular layer (*IML*) of the dentate gyrus in AD. Chromogranin B-immunopositive plaques are already seen in an overview in the molecular layer of the dentate gyrus (*IML*, indicated by *arrowheads*) (*AD* Alzheimer's disease, *PL* polymorphic layer of the dentate gyrus). *Bars* **A**, **B** 500 μm

Fig. 3 Chromogranin B-LI in the entorhinal cortex in controls (**A**) ▶ and in AD (**B**). A high density of chromogranin B-LI is detected in layers II, III and V in controls. Chromogranin B-LI is significantly reduced in these layers in AD (**B**). In controls, a high density of chromogranin B-LI is present in the inner molecular layer of the dentate gyrus (*IML*, **C**). In AD chromogranin B-LI is significantly reduced in this layer (**D**). A chromogranin B-immunoreactive plaque is present in the outer molecular layer (*OML*, indicated by *arrowheads*). *Bars* **A**, **B** 50 μm, **C**, **D** 300 μm

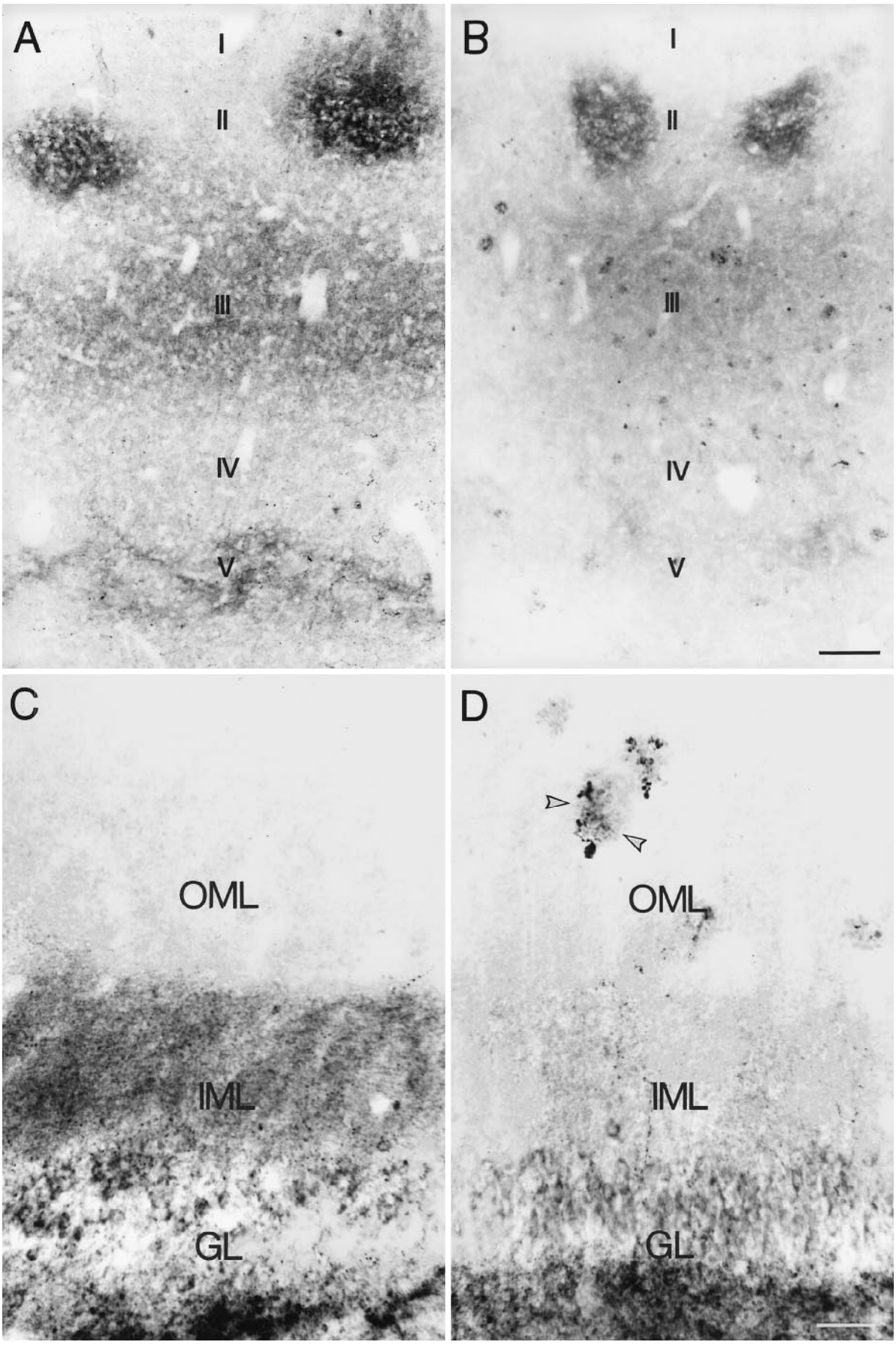
A
I
II
III
IV
V
B
I
II
III
IV
V
C
OML
IML
GL
D
OML
IML
GL

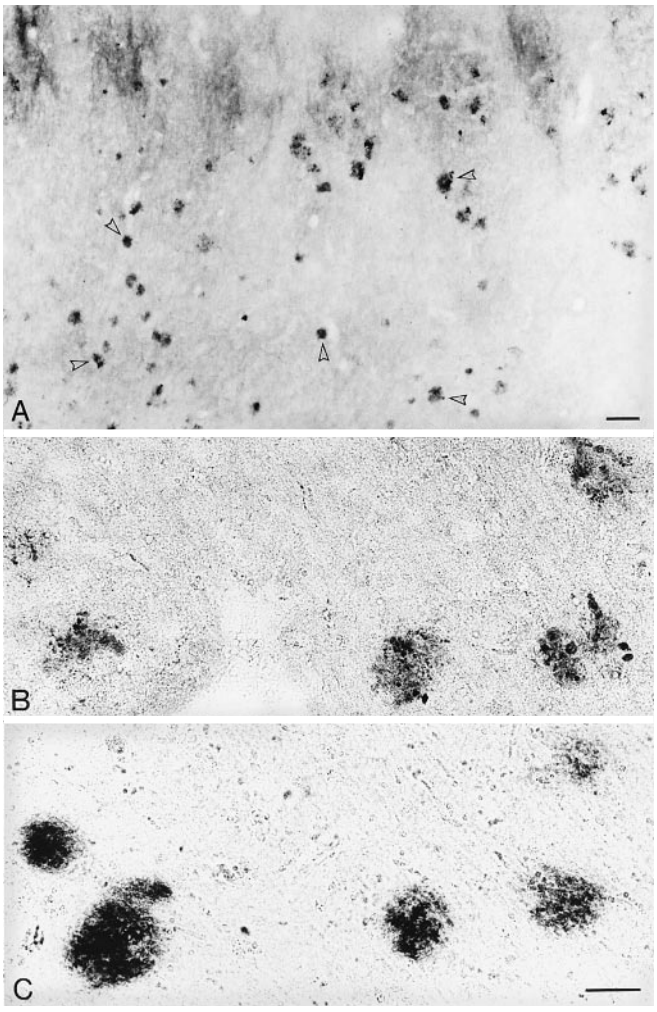

Fig. 4 Chromogranin B-LI in the subiculum in AD. At a late stage of the disease numerous chromogranin B-immunoreactive plaques are observed throughout all layers (some plaques are indicated by *arrowheads*; **A**). Chromogranin B-immunopositive plaques (**B**) are co-localizing with amyloid-immunoreactive plaques (**C**). Bar **A** 100 μm, **C** (also for **B**) 50 μm

20% of the amyloid-stained plaques were chromogranin B immunopositive. In parts of the entorhinal cortex and subiculum, the degree of overlap between chromogranin B- and amyloid-immunopositive plaques was higher (Fig. 4 B, C). Diffusely chromogranin B-immunopositive plaques were also present.

In the examined areas (Fig. 5), a decrease of chromogranin B-LI, as revealed by a decrease in the mean optical density, was observed in the inner molecular layer (by about 82%; $P < 0.01$), stratum lucidum of the CA3 subregion (by about 46%, $P < 0.01$), layer II of the entorhinal cortex (by about 26%; $P < 0.05$); layer III of the entorhinal cortex (by about 43%; $P < 0.01$), layer V of the entorhinal cortex (by about 40%; $P < 0.01$). No significant decrease of chromogranin B-LI was found in the polymorphic layer of the dentate gyrus, in the outer molecular layer of the dentate gyrus, or in layer IV and VI of the entorhinal cortex.

Loss of chromogranin B-LI was especially evident in paraffin sections (not shown) which were thinner than the free floating sections (3 μm and 40 μm, respectively). Incubations with a PE-11 antibody dilution of 1:600 revealed numerous immunoreactive varicosities in the inner molecular layer of controls, whereas only a few varicosities were detected in AD brains.

Discussion

Distribution of chromogranin B-LI in controls

The present study shows that chromogranin B-LI is distinctly distributed in the human hippocampal formation and entorhinal cortex. It is particularly abundant in the terminal field of mossy fibers and the inner molecular layer of the dentate gyrus. Comparison of the chromogranin B immunostaining with that of chromogranin A, another member of the chromogranin family, shows differences in their distribution pattern. Chromogranin A is

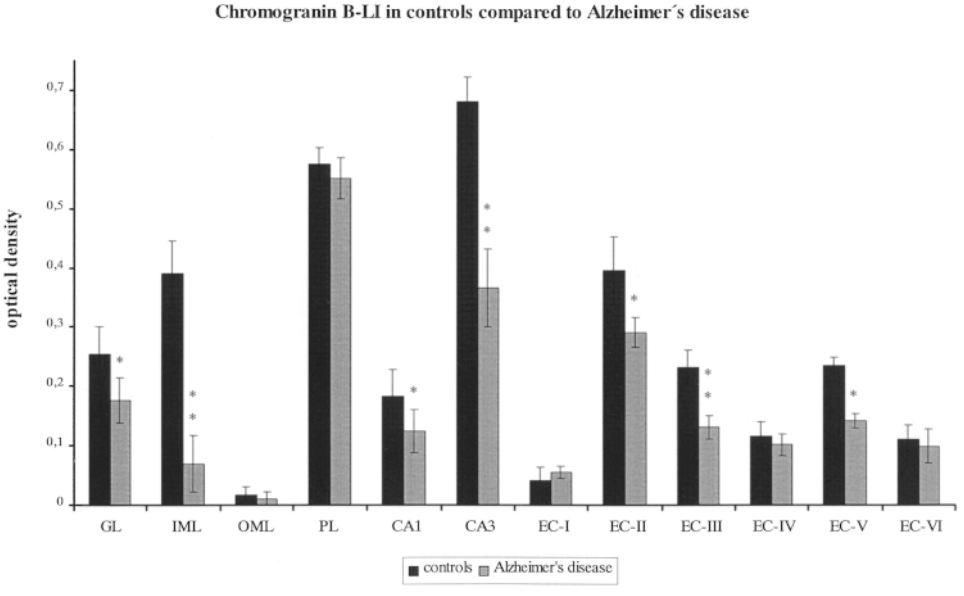

Fig. 5 The regional distribution of optical density values in the hippocampal formation in controls and AD; *bars* represent mean optical density ± SEM (see Material and methods) (*GL* granule cell layer, *IML* inner molecular layer, *OML* outer molecular layer, *PL* polymorphic layer of the dentate gyrus, *EC* entorhinal cortex). *$P < 0.05$, **$P < 0.01$

concentrated in the mossy fiber system and the CA2 sector [29], whereas the molecular layer of the dentate gyrus displays, in contrast to the chromogranin B system, a low density of chromogranin A-LI. Secretoneurin, a peptide deriving from secretogranin II, is concentrated in the innermost part of the inner molecular layer [19]. Therefore, the differential localization of secretoneurin- and chromogranin B-LI is particularly suitable for detecting synaptic changes in the inner molecular layer of the dentate gyrus.

Chromogranin B-LI in AD

In controls, there was no obvious age- or sex-related difference in the chromogranin B-LI distribution pattern. Keeping the limitations of quantitative results in mind, a significant loss of chromogranin B-immunoreactivity was found in AD brains when compared to controls. The loss of chromogranin B-immunoreactivity was particularly obvious in 3-μm-thick sections.

Synaptic pathology in AD involves the whole synapse since different synaptic vesicle proteins (rab3a, synaptotagmin, synaptophysin) and also the presynaptic membrane protein GAP-43 and the postsynaptic protein neurogranin are reduced [5]. In a previous study, a loss of secretogranin II-LI, the precursor of secretoneurin, was found in total hippocampus [23]. In the same study, levels of chromogranin A were increased. Chromogranin A was not investigated in the present study; therefore, co-localization studies are necessary both to reveal the degree of co-localization between chromogranin A, chromogranin B and secretoneurin and to clarify whether co-localized vesicle markers are differentially regulated. Secretoneurin was also reduced in the innermost part of the inner molecular layer of the dentate gyrus in severe AD [19]. Loss of synaptophysin was reported with no spatial relationship to plaques and tangles [13]. Furthermore, immunoblotting revealed a loss of about 20–30% for synaptophysin, SVII and synaptotagmin [23]. For synaptophysin, a decrease in immunoreactivity was also shown in immunocytochemical studies [26]. Western analysis showed that in AD levels of synaptobrevin and synaptophysin were decreased by about 30% from amounts in controls, while those of synaptotagmin, synaptosomal-associated protein 25, and syntaxin were decreased by only about 10% [32]. As synaptobrevin and synaptophysin are localized mainly in transmitter-containing synaptic vesicles, whereas synaptosomal-associated protein 25 and syntaxin are found in presynaptic plasma membranes, a differential involvement of synaptic components may occur in AD.

In AD brain, a decline of synapses was also shown in the inner molecular layer of the dentate gyrus at the ultrastructural level. This decline was accompanied by a significant increase in apposition length and resulted in a significant correlation with the synaptic density [31].

In the entorhinal cortex, there is a correlation between the decrease of chromogranin B-LI and the number of neuritic plaques. This area also displays the highest number of chromogranin B and amyloid co-labeling plaques. The marked alterations in different layers of the entorhinal cortex are likely to be responsible for the disruption of the modular organization of the entorhinal cortex [33] and its effect on memory-related neural systems. In this area, a subset of Aβ-deposits has been shown to contribute directly to neural system failure in AD [21].

Functional implications

Chromogranins are a family of regulated secretory proteins. Their aggregation is promoted by calcium ions and low pH. These two parameters are important in the trans-Golgi network. There is now increasing evidence that chromogranins play an important role for sorting to the secretory granules [35]. In the case of chromogranin B, reduction of the disulfide bond is sufficient to cause complete missorting of constitutive secretory vesicles [4]. Therefore, our experiments showing changes in chromogranin tissue levels may be of importance for the sorting of vesicles. Another important aspect is the capability of chromogranin-derived peptides to influence release of other vesicle constituents [4]. Therefore, decreased chromogranin B concentrations may have important functional implications.

Conclusion

The present study demonstrates that chromogranin B is a marker in human hippocampal pathways. It is particularly suitable for studying nerve fibers ending at the inner part of the molecular layer of the dentate gyrus and in different layers of the entorhinal cortex. Chromogranin B is present in neuritic plaques, and its density is reduced in a layer-specific manner. Therefore, chromogranin B is a suitable marker for synaptic changes in AD.

Acknowledgements J. Marksteiner was supported by the Austrian National Bank (7150). The excellent technical assistance by R. Moser is gratefully acknowledged.

References

1. Behan DP, Khongsaly O, Owens MJ, Chung HD, Nemeroff CB, De Souza EB (1997) Corticotropin-releasing factor (CRF), CRF-binding protein (CRF-BP), and CRF/CRF-BP complex in Alzheimer's disease and control postmortem human brain. J Neurochem 68: 2053–2060
2. Benjannet S, Leduc R, Adrouche N, Falgueyret JP, Marcinkiewicz M, Seidah NG, Mbikay M, Lazure C, Chretien M (1987) Chromogranin B (secretogranin I), a putative precursor of two novel pituitary peptides through processing at paired basic residues. FEBS Lett 224: 142–148
3. Braak H, Braak E (1991) Neuropathological stageing of Alzheimer-related changes. Acta Neuropathol 82: 239–259
4. Chanat E, Weiss U, Huttner WB, Tooze SA (1993) Reduction of the disulfide bond of chromogranin B (secretogranin I) in the trans-Golgi network causes its missorting to the constitutive secretory pathways. EMBO J 12: 2159–2168

5. Davidsson P, Blennow K (1998) Neurochemical dissection of synaptic pathology in Alzheimer's disease. Int Psychogeriatr 10: 11–23
6. Davis KL, Mohs RC, Marin DB, Purohit DP, Perl DP, Lantz M, Austin G, Haroutunian V (1999) Neuropeptide abnormalities in patients with early Alzheimer disease. Arch Gen Psychiatry 56: 981–987
7. Dickson DW, Crystal HA, Bevona C, Honer W, Vincent I, Davies P (1995) Correlations of synaptic and pathological markers with cognition of the elderly. Neurobiol Aging 16: 285–298
8. Erickson JD, Lloyd R, Trojanowski JQ, Iacangelo A, Eiden E (1992) Sites of synthesis of chromogranins A and B in the human brain. Neuropeptides 21: 239–244
9. Fischer-Colbrie R, Hagn C, Schober M (1987) Chromogranins A, B, and C: widespread constituents of secretory vesicles. Ann N Y Acad Sci 493: 120–134
10. Folstein MF, Folstein SE, McHugh PR (1975) "Mini-mental state". A practical method for grading the cognitive state of patients for the clinician. J Psychiatr Res 12: 189–198
11. Forss-Petter S, Danielson P, Battenberg E, Bloom F, Sutcliffe JG (1989) Nucleotide sequence and cellular distribution of rat chromogranin B (secretogranin I) mRNA. J Mol Neurosci 1: 63–75
12. Gabriel SM, Davidson M, Haroutunian V, Powchik P, Bierer LM, Purohit DP, Perl DP, Davis KL (1996) Neuropeptide deficits in schizophrenia vs Alzheimer's disease cerebral cortex. Biol Psychiatry 39: 82–91
13. Heinonen O, Soininen H, Sorvari H, Kosunen O, Paljarvi L, Koivisto E, Riekkinen PJS (1995) Loss of synaptophysin-like immunoreactivity in the hippocampal formation is an early phenomenon in Alzheimer's disease. Neuroscience 64: 375–384
14. Husain MM, Nemeroff CB (1990) Neuropeptides and Alzheimer's disease. J Am Geriatr Soc 38: 918–925
15. Huttner WB, Gerdes HH, Rosa P (1991) The granin (chromogranin/secretogranin) family. Trends Biochem Sci 16: 27–30
16. Hyman BT (1998) New neuropathological criteria for Alzheimer disease [editorial]. Arch Neurol 55: 1174–1176
17. Jellinger KA (1997) Neuropathological staging of Alzheimer-related lesions: the challenge of establishing relations to age. Neurobiol Aging 18: 369–375
18. Jellinger KA, Bancher C (1998) Neuropathology of Alzheimer's disease: a critical update. J Neural Transm Suppl 54: 77–95
19. Kaufmann WA, Barnas U, Humpel C, Nowakowski K, DeCol C, Gurka P, Ransmayr G, Hinterhuber H, Winkler H, Marksteiner J (1998) Synaptic loss reflected by secretoneurin-like immunoreactivity in the human hippocampus in Alzheimers disease. Eur J Neurosci 10: 1084–1094
20. Khachaturian ZS (1985) Diagnosis of Alzheimer's disease. Arch Neurol 42: 1097–1105
21. Knowles RB, Gomez-Isla T, Hyman BT (1998) Aβ associated neuropil changes: correlation with neuronal loss and dementia. J Neuropathol Exp Neurol 57: 1122–1130
22. Kroesen S, Marksteiner J, Leitner B, Hogue Angeletti R, Fischer Colbrie R, Winkler H (1996) Rat brain: distribution of immunoreactivity of PE-11, a peptide derived from chromogranin B. Eur J Neurosci 8: 2679–2689
23. Lassmann H, Weiler R, Fischer P, Bancher C, Jellinger K, Floor E, Danielczyk W, Seitelberger F, Winkler H (1992) Synaptic pathology in Alzheimer's disease: immunological data for markers of synaptic and large dense-core vesicles. Neuroscience 46: 1–8
24. Marcinkiewicz M, Benjannet S, Seidah NG, Cantin M, Chrétien M (1985) Immunocytochemical localization of a novel pituitary protein (7B2) within the rat brain and hypophysis. J Histochem Cytochem 33: 1219–1226
25. Marksteiner J, Bauer R, Kaufmann WA, Weiss E, Barnas U, Maier J (1999) PE-11, a peptide derived from chromogranin B, in the human brain. Neuroscience 91: 1155–1170
26. Masliah E, Terry RD, Alford M, DeTeresa R, Hansen LA (1991) Cortical and subcortical patterns of synaptophysinlike immunoreactivity in Alzheimer's disease. Am J Pathol 138: 235–246
27. McKhann G, Drachman D, Folstein M, Katzman R, Price D, Stadlan EM (1984) Clinical diagnosis of Alzheimer's disease: report of the NINCDS-ADRDA Work Group under the auspices of Department of Health and Human Services Task Force on Alzheimer's Disease. Neurology 34: 939–944
28. Mirra SS, Heyman A, McKeel D, Sumi SM, Crain BJ, Brownlee LM, Vogel FS, Hughes JP, Belle G van, Berg L (1991) The consortium to establish a registry for Alzheimer's disease. Neurology 41: 479–486
29. Munoz DG (1990) The distribution of chromogranin A-like immunoreactivity in the human hippocampus coincides with the pattern of resistance to epilepsy-induced neuronal damage. Ann Neurol 27: 266–275
30. Reisberg B, Ferris SH, De Leon MJ, Crook T (1982) The Global Deterioration Scale for assessment of primary degenerative dementia. Am J Psychiatry 139: 1136–1139
31. Scheff SW, Price DA (1998) Synaptic density in the inner molecular layer of the hippocampal dentate gyrus in Alzheimer disease. J Neuropathol Exp Neurol 57: 1146–1153
32. Shimohama S, Kamiya S, Taniguchi T, Akagawa K, Kimura J (1997) Differential involvement of synaptic vesicle and presynaptic plasma membrane proteins in Alzheimer's disease. Biochem Biophys Res Commun 236: 239–242
33. Solodkin A, Van Hoesen GW (1996) Entorhinal cortex modules of the human brain. J Comp Neurol 365: 610–617
34. Sunderland T, Rubinow DR, Tariot PN, Cohen RM, Newhouse PA, Mellow AM, Mueller EA, Murphy DL (1987) CSF somatostatin in patients with Alzheimer's disease, older depressed patients, and age-matched control subjects. Am J Psychiatry 144: 1313–1316
35. Thiele C, Huttner WB (1998) The disulfide-bonded loop of chromogranins, which is essential for sorting to secretory granules, mediates homodimerization. J Biol Chem 273: 1223–1231
36. Tierney MC, Fisher RH, Lewis ASJ, Zorzitto ML, Snow WG, Reid DW, Nieuwstraten P (1988) The NINCDS-ADRDA Work Group criteria for the clinical diagnosis of probable Alzheimer's disease: a clinicopathologic study of 57 cases. Neurology 38: 359–364
37. Zwieten EJ van, Ravid R, Swaab DF (1996) Differential vasopressin and oxytocin innervation of the human parabrachial nucleus: no changes in Alzheimer's disease. Brain Res 711: 146–152